

Supporting Information for

A Simple Method for Floating Graphene Oxide Films Facilitates Nanoscale Investigations of Ion and Water Adsorption

*Raju R. Kumal, Amanda J. Carr, and Ahmet Uysal**

Chemical Sciences and Engineering Division, Argonne National Laboratory, Lemont, IL 60439, United States

*Corresponding Author: ahmet@anl.gov

§Present Address: Fresenius Kabi USA, 2020 N. Ruby Street, Melrose Park, IL 60160, USA

1. GO membrane fabrication

Thicker GO membranes were fabricated for XPS, and FTIR analysis as follows. Stock solutions of GO-1, GO-2, and GO-3 were briefly sonicated for 10 minutes. GO-2 (2 mg/mL) and GO-3 (10 mg/mL) were each diluted to 1 mg/mL using ultra-pure water. Each sample was diluted again 5:1 v:v methanol:sample and sonicated for 1 hour. Samples were filtered using a 1.2 µm syringe filter. GO membranes were prepared using vacuum filtration by diluting each prepared sample 5:1 v:v sample:water and sonicating for 15 minutes. The solution was placed on a clean, sterilized polyvinylidene fluoride (PVDF) support membrane (Sigma Aldrich, USA) with a nominal pore size of 220 nm and vacuum filtered until no solution remained. The resulting membranes varied in color from light gray to brown.

2. X-ray photoelectron spectroscopy (XPS)

X-ray photoelectron spectroscopy (XPS, Thermo Scientific ESCALAB 250Xi) was completed on fabricated GO membranes. Survey scans from 0 – 1200 eV with a 1 eV step size (Figure S1) and high resolution scans of C 1s (Figure S3), O 1s (Figure S4), S 2p (Figure S5), and F 1s (Figure S6) regions were completed for each GO. All data were offset calibrated such that the O=C-OH peak of the C 1s high resolution scan appeared at 289.2 eV.¹ The survey scans showed the expected carbon and oxygen signals. GO-1 also showed significant F signal, attributed to the underlying PVDF substrate. The atomic compositions of each sample were determined (Table S1). The C/O ratios were calculated for each sample as follows. Note that carbon signal associated with the PVDF substrate was subtracted for GO-1. The determined C/O ratios are: 43.1% C/11.3% O = 3.81 for GO-1; 71.4% C/28.2% O = 2.53 for GO-2; and 74.6% C/24.9% O = 3.00 for GO-3. The oxygen content for GO-1 agrees with the information

provided by the manufacturer² but the determined oxygen contents of GO-2³ and GO-3⁴ are significantly lower than those provided by the manufacturers.

High resolution data were fitted with Lorentzian peakshapes after Shirley background subtraction in CasaXPS.⁵ Peak assignments were made as follows. Fitted peak centers are provided in Table S2. For the C1s region,¹ 285 eV corresponds to C-C, C=C, and C-H bonds, noting that XPS cannot reliably differentiate between these 3 bonding environments; 287 eV corresponded to C-O-C and C-OH bonds, again noting that the core electron energy differences between C-O-C and C-OH cannot reasonably be distinguished using XPS; 289.2 eV corresponds to O=C-OH bonds (used as a calibration offset); and 292 eV corresponds to C-F bonds. This C-F bonding environment is attributed to the PVDF substrate and is only present in GO-1, indicating the formed membrane was thin and allowed detection of the underlying substrate. For the O 1s region, 532 was assigned to O, which may be HO-C and/or O=C.⁶ For the S 2p region, 169 eV corresponds to S,⁷ a common contaminate in GO fabricated via Hummers synthesis,⁸ present in both GO-2 and GO-3. For the F1s region, 684 eV corresponds to F-C-F and 687 eV corresponds to F-C, referring to the main chain units and tail units of PVDF, respectively.⁹ Interestingly, the F1s region of GO-1 is shifted higher in energy, possibly because more of the substrate was detected.

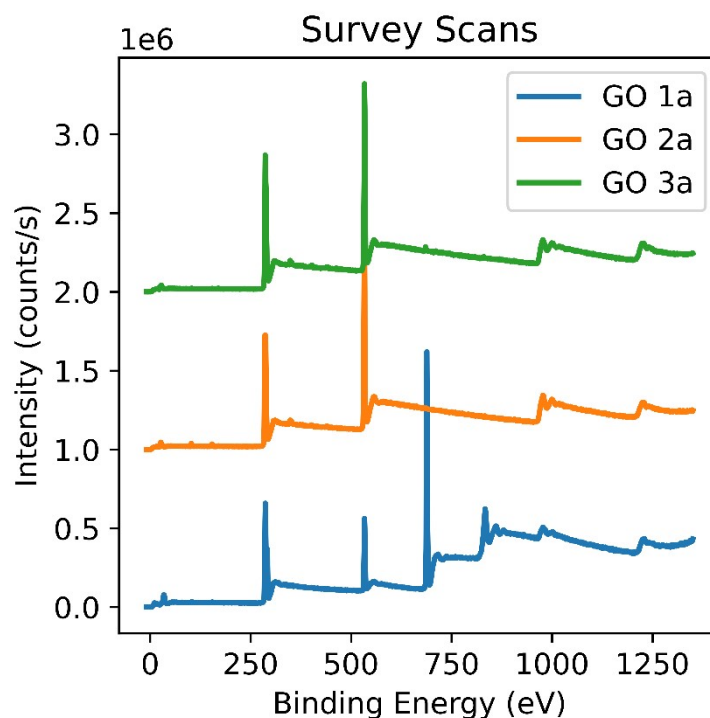


Figure S1. XPS survey scans of GO membranes on PVDF support substrates.

Table S1. Atomic compositions of each GO as determined from the survey XPS scans

| Sample | Atomic % C | Atomic % O | Atomic % S | Atomic % F |
|--------|------------|------------|------------|------------|
| GO-1 | 65.9 | 11.3 | 0.00 | 22.8 |
| GO-2 | 71.4 | 28.2 | 0.21 | 0.11 |
| GO-3 | 74.6 | 24.9 | 0.18 | 0.30 |

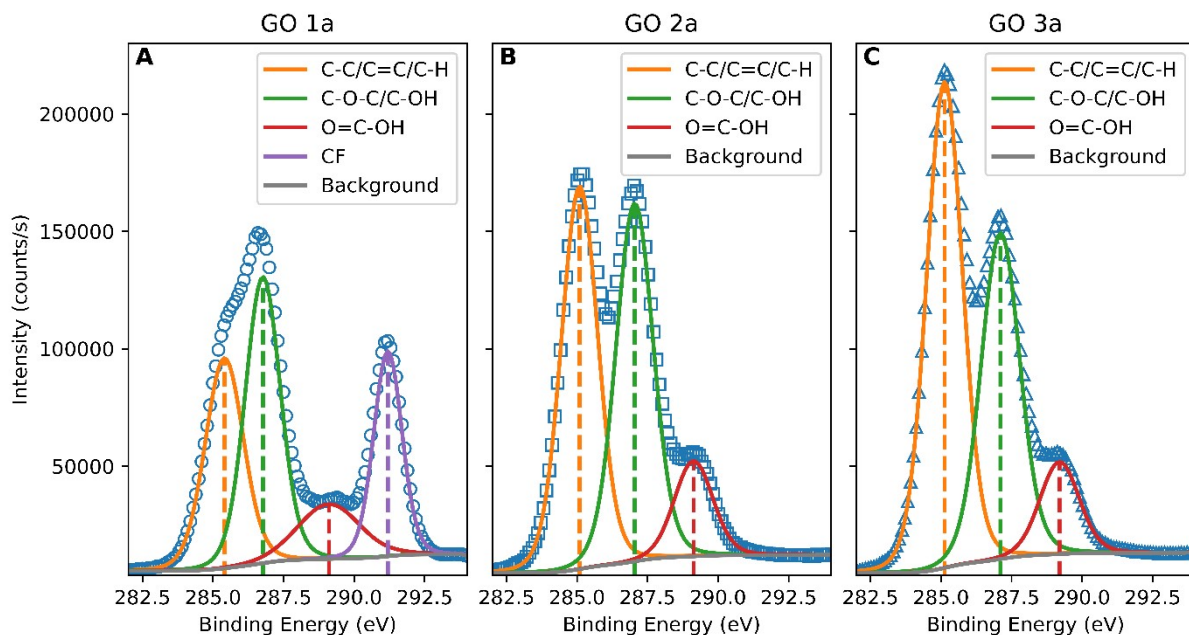


Figure S2. High-resolution XPS scans of the C 1s region of GO membranes on PVDF support substrates.

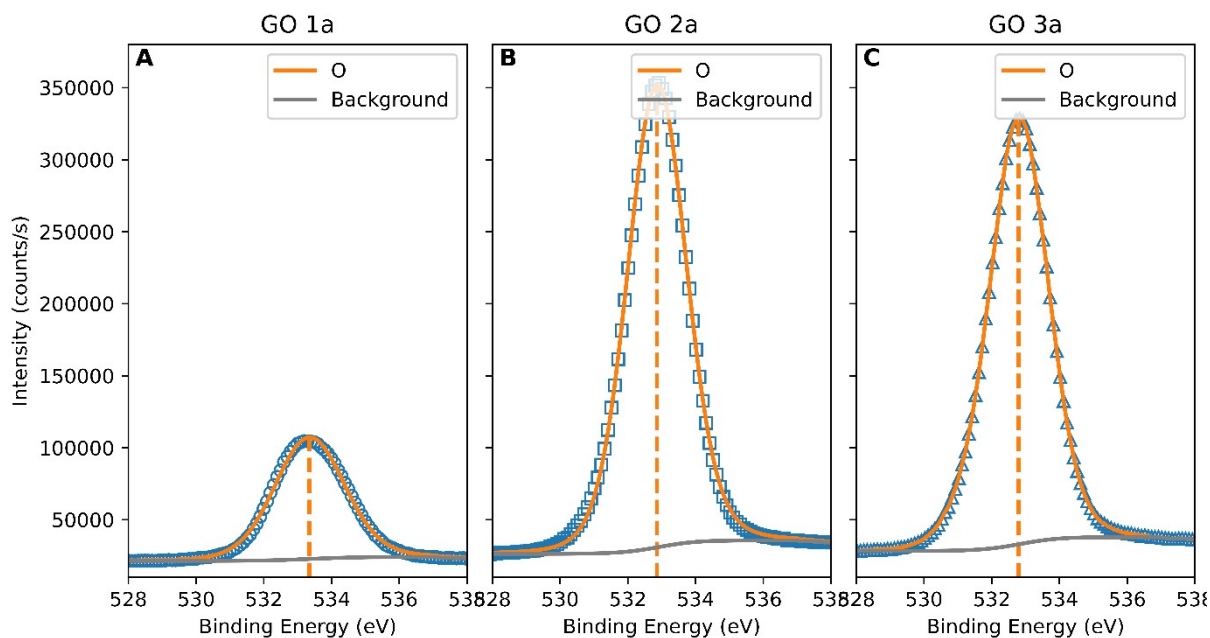


Figure S3. High-resolution XPS scans of the O 1s region of GO membranes on PVDF support substrates.

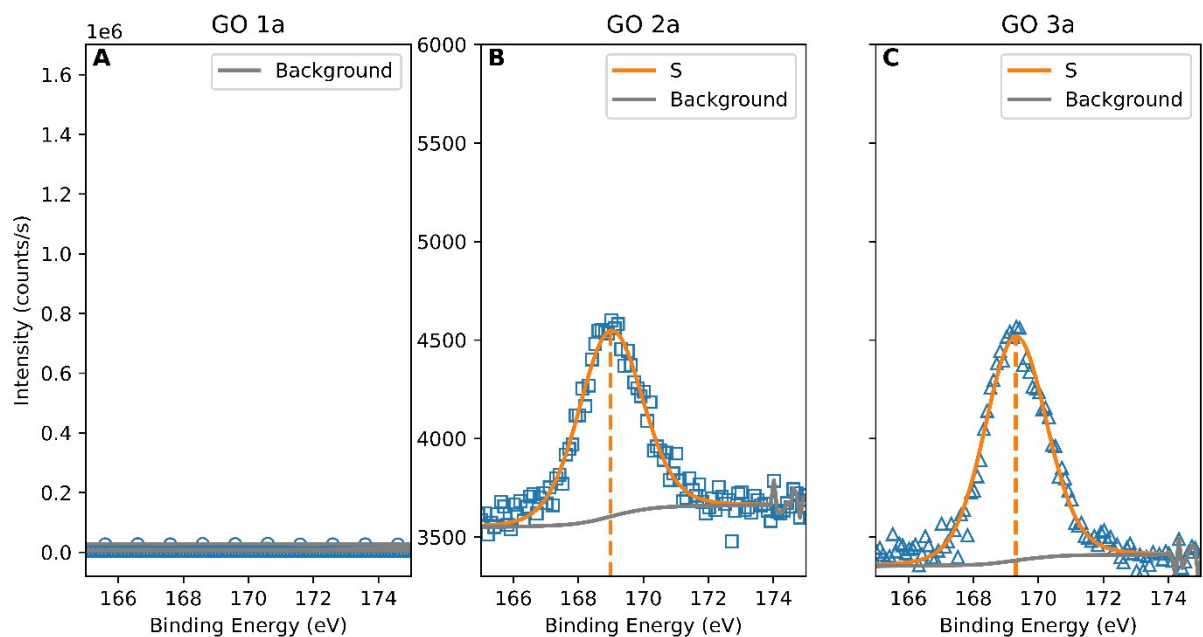


Figure S4. High-resolution XPS scans of the S 2p region of GO membranes on PVDF support substrates.

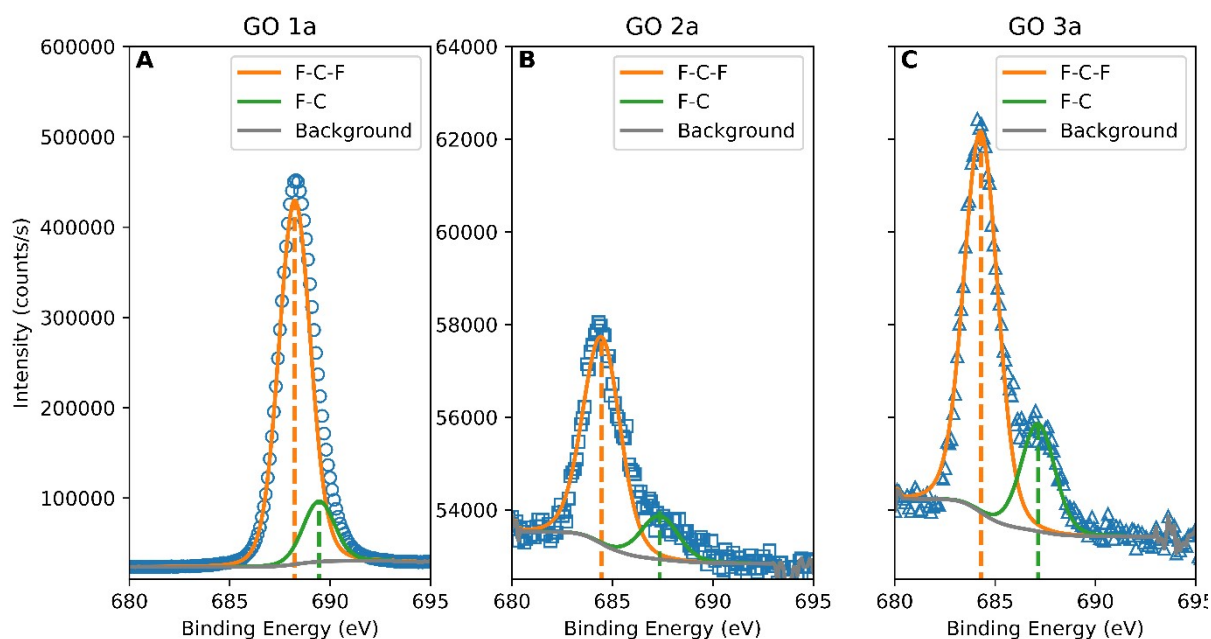


Figure S5. High-resolution XPS scans of the F 1s region of GO membranes on PVDF support substrates.

Table S2. Fitted peak positions of each GO as determined from high resolution XPS scans

| Region | Assignment | GO-1 Fitted peak position (eV) | GO-2 Fitted peak position (eV) | GO-3 Fitted peak position (eV) |
|--------|---------------|--------------------------------------|--------------------------------------|--------------------------------------|
| C1s | C-C/C=C/C-H | 285.4 | 285.1 | 285.1 |
| | C-O-C/C-OH | 286.8 | 287.0 | 287.1 |
| | O=C-OH | 289.1 | 289.1 | 289.2 |
| | C-F | 291.2 | -- | -- |
| O1s | O (O=C, HO-C) | 533.3 | 532.9 | 532.8 |
| S2p | S | -- | 169.0 | 169.3 |
| F1s | F-C-F | 688.2 | 684.5 | 684.3 |
| | F-C | 689.4 | 687.4 | 687.1 |

3. FTIR analysis

AT-FTIR (Thermo Scientific Nicolet iS50, 4 cm^{-1} , 64 scans) spectroscopy was also completed on the prepared GO membranes (Figure S6). The peaks were assigned as follows:¹⁰ 1050 and 1170 cm^{-1} correspond to the C-O stretching modes for different alcohols; 1230 cm^{-1} corresponds to the C-O-C epoxide stretching mode; 1400 cm^{-1} corresponds to the C-F stretching mode, likely from the PVDF support substrate; 1630 cm^{-1} corresponds to the C=C stretching mode; 1740 cm^{-1} corresponds to the C=O carbonyl stretching mode; 2850, 2920, and 2960 cm^{-1} correspond to C-H stretching modes for different carbon chains; and the broad band from 3000 – 3700 cm^{-1} corresponds to O-H stretching, likely from both hydroxide groups on the GO and water.

The variation of peak intensities for each GO sample suggests the compositions differ, in agreement with the previous XPS analysis. The GO-1 peak intensities and shapes generally differ from those of GO-2 and GO-3, which are more similar to each other. Similarly, GO-2 and GO-3 have larger peak intensities for the alcohol and carbonyl stretches, suggesting more oxygen-containing functional groups compared to GO-1.

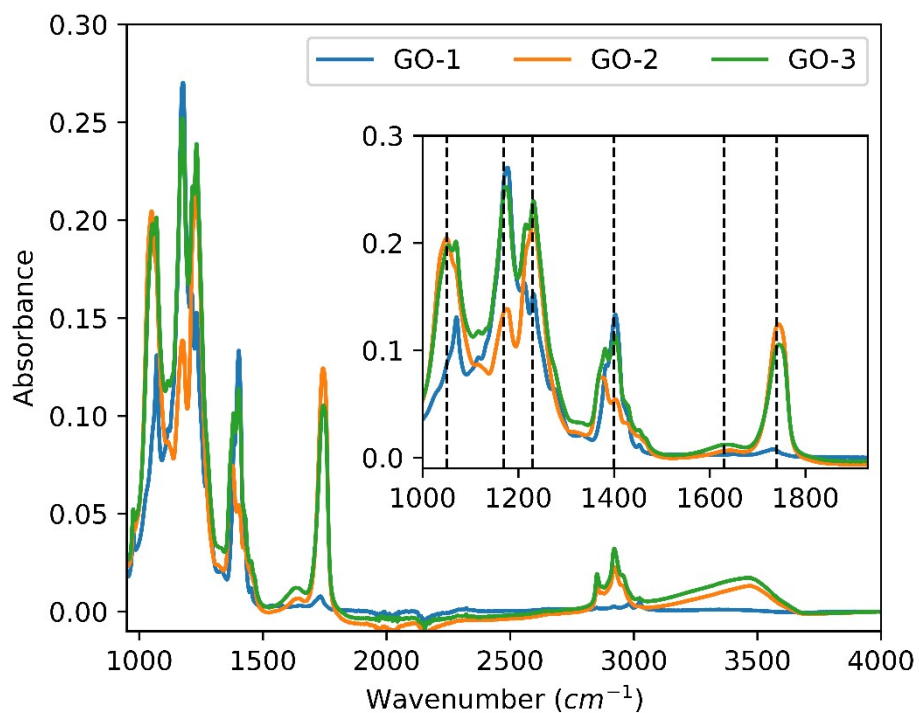


Figure S6. FTIR (A) spectroscopy of GO membranes on PVDF support substrates.

4. Surface pressure analysis

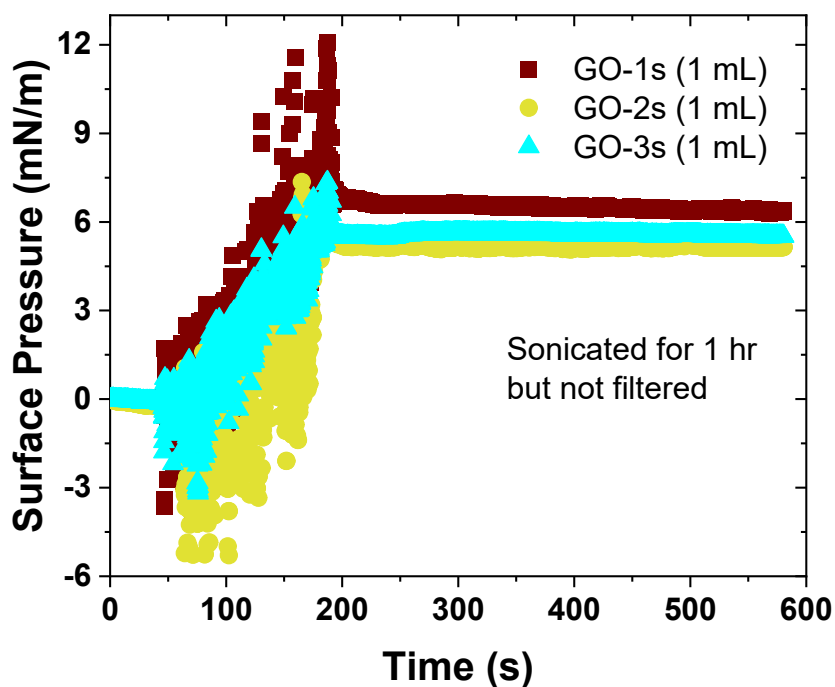


Figure S7. Surface pressure of GO samples that are sonicated for 1 hour but not filtered. The poor surface pressure indicates that the sonication of sample itself doesn't form a good film, filtration is essential.

5. Supplemental SFG data and fits

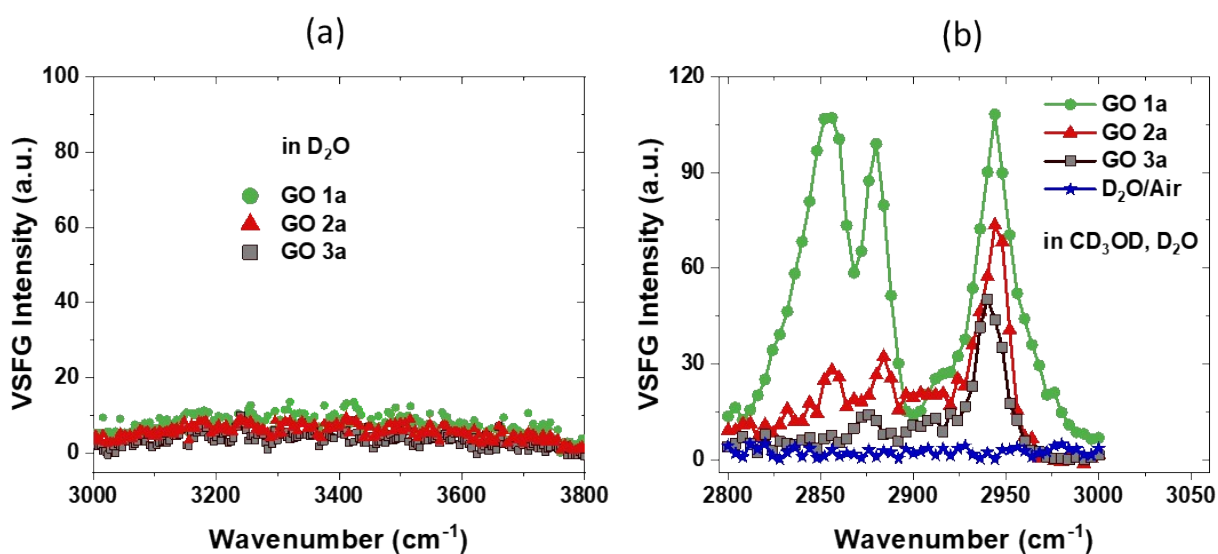


Figure S8. (a) OH-stretch region of different GO films. Here, the GO is suspended in a deuterated system consisting of 1:5 mixture of D₂O and deuterated methanol (CD₃OD). The absence of 3640 cm⁻¹ band in this deuterated system suggests that this peak (Figure 2b-d) is not originated from the functional group -OH of the GO films rather due to the water molecules interacting with GO layers. And (b) the VSFG intensities of CH-stretch region of various GO films prepared in a deuterated system (CD₃OD and D₂O), and the intensity D₂O/air interface as a reference.

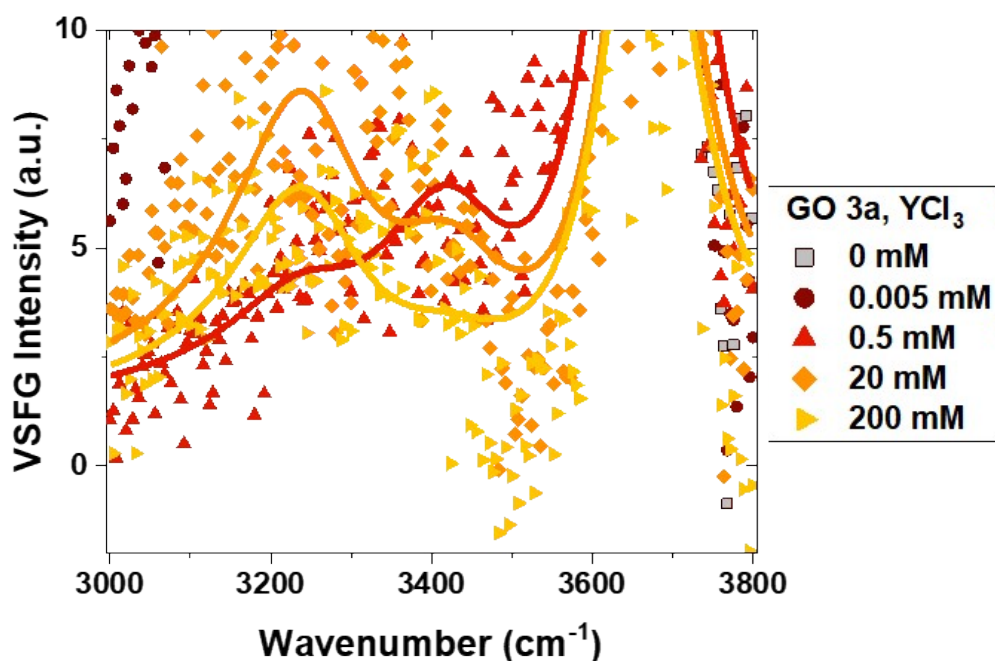


Figure S9. Zoomed in plot of Figure 2c.

Table S3. Fit parameters of OH-stretch region of GO/water and air/water interface (Figure 2b). Experiment data obtained for GO-1a, GO-2a, and GO-3a are fitted globally. The experiment data obtained for GO-3b and air/water interfaces are fitted individually.

| Fit Parameters | | Sample | | | | |
|---------------------------------------|----------------|------------|----------|----------|--------------|----------------------|
| | | GO-1a | GO-2a | GO-3a | GO-3b | Air/H ₂ O |
| A _n | A ₁ | 344 ± 27 | 459 ± 32 | 561 ± 35 | 169 ± 81 | 160 ± 65 |
| | A ₂ | 484 ± 33 | 463 ± 24 | 550 ± 22 | 200 ± 109 | 130 ± 55 |
| | A ₃ | 174 ± 25 | 163 ± 44 | 148 ± 42 | 38 ± 8 | 42 ± 5 |
| ω _v (cm ⁻¹) | ω ₁ | 3250 ± 4 | | | 3265 ± 9 | 3228 ± 11 |
| | ω ₂ | 3440 ± 7 | | | 3411 ± 9 | 3360 ± 9 |
| | ω ₃ | 3640 ± 10 | | | 3706 ± 2 | 3704 ± 1 |
| Γ _v (cm ⁻¹) | Γ ₁ | 100 ± 18 | | | 76 ± 22 | 90 ± 29 |
| | Γ ₂ | 100 ± 17 | | | 84 ± 26 | 79 ± 29 |
| | Γ ₃ | 70 ± 21 | | | 10 ± 2 | 10 ± 1 |
| χ _{NR} ⁽²⁾ | | -1.8 ± 0.2 | | | -0.49 ± 0.29 | -0.45 ± 0.4 |

Table S4. Fit parameters of OH-stretch region of GO-3a/water interface at different YCl₃ concentrations (Figure 2c). Experimentally obtained data are fitted globally.

| Fit Parameters | | GO-3a_YCl ₃ Concentrations | | | | | | |
|---------------------------------------|----------------|---------------------------------------|----------|----------|----------|----------|----------|----------|
| | | 0 mM | 0.005 mM | 0.5 mM | 2 mM | 20 mM | 100 mM | 200 mM |
| A _n | A ₁ | 613 ± 41 | 380 ± 31 | 48 ± 25 | 48 ± 27 | 152 ± 23 | 145 ± 25 | 127 ± 26 |
| | A ₂ | 597 ± 22 | 497 ± 48 | 101 ± 27 | 58 ± 29 | 78 ± 32 | 11 ± 35 | 34 ± 33 |
| | A ₃ | 75 ± 16 | 157 ± 22 | 245 ± 32 | 232 ± 31 | 193 ± 28 | 195 ± 29 | 190 ± 28 |
| ω _v (cm ⁻¹) | ω ₁ | 3248 ± 3 | | | | | | |
| | ω ₂ | 3427 ± 2 | | | | | | |
| | ω ₃ | 3667 ± 3 | | | | | | |
| Γ _v (cm ⁻¹) | Γ ₁ | 100 ± 16 | | | | | | |
| | Γ ₂ | 100 ± 31 | | | | | | |
| | Γ ₃ | 68 ± 5 | | | | | | |
| χ _{NR} ⁽²⁾ | | 1.0 ± 0.3 | | | | | | |

Table S5. Fit parameters of OH-stretch region of GO/water interfaces at 20 mM YCl_3 concentration (Figure 2d). Experimentally obtained data are fitted globally.

| Fit Parameters | | 20 mM YCl_3 | | |
|------------------------------------|------------|----------------------|-------------|--------------|
| | | GO-1a | GO-2a | GO-3a |
| A_n | A_1 | 10 ± 7 | 89 ± 12 | 240 ± 12 |
| | A_2 | 300 ± 14 | 21 ± 10 | 74 ± 8 |
| | A_3 | 196 ± 5 | 221 ± 5 | 173 ± 12 |
| ω_v (cm^{-1}) | ω_1 | 3165 ± 7 | | |
| | ω_2 | 3400 ± 8 | | |
| | ω_3 | 3623 ± 4 | | |
| Γ_v (cm^{-1}) | Γ_1 | 138 ± 8 | | |
| | Γ_2 | 139 ± 6 | | |
| | Γ_3 | 80 ± 5 | | |
| $\chi_{\text{NR}}^{(2)}$ | | 1.2 ± 0.2 | | |

Table S6. Fit parameters of OD-stretch region of GO/ D_2O and air/ D_2O interfaces (Figure 2f). Experimentally obtained data are fitted globally.

| Fit Parameters | | Sample | | | |
|------------------------------------|------------|---------------|--------------|--------------|---------------------------|
| | | GO-1a | GO-2a | GO-3a | Air/ D_2O |
| A_n | A_1 | 242 ± 17 | 286 ± 22 | 278 ± 25 | 41 ± 8 |
| | A_2 | 127 ± 13 | 116 ± 14 | 150 ± 12 | 40 ± 1 |
| | A_3 | 0.3 ± 5 | 0.3 ± 4 | 0.5 ± 2 | 16 ± 2 |
| ω_v (cm^{-1}) | ω_1 | 2356 ± 6 | | | 2347 ± 4 |
| | ω_2 | 2453 ± 5 | | | 2460 ± 4 |
| | ω_3 | 2711 ± 2 | | | 2743 ± 1 |
| Γ_v (cm^{-1}) | Γ_1 | 49 ± 8 | | | 38 ± 7 |
| | Γ_2 | 48 ± 7 | | | 38 ± 8 |
| | Γ_3 | 1 ± 1 | | | 7 ± 1 |
| $\chi_{\text{NR}}^{(2)}$ | | 1.8 ± 0.1 | | | 1.3 ± 0.1 |

6. XR fit parameters

Table S7. X-ray reflectivity fit parameters. The GO 3a and GO 2a are fitted using a three-box model. The GO 3b is fitted using a one-box model.

| | Region I | | Region II | | Region III | | |
|--------|----------------|-----------------------------|---------------|-----------------------------|----------------|-----------------------------|-----------------|
| Sample | d_1 (Å) | ρ_1 ($e/\text{Å}^3$) | d_2 (Å) | ρ_2 ($e/\text{Å}^3$) | d_3 (Å) | ρ_3 ($e/\text{Å}^3$) | σ (Å) |
| GO 3a | 17.5 ± 0.2 | 0.366 ± 0.001 | 9.7 ± 0.1 | 0.503 ± 0.009 | 10.7 ± 0.1 | 0.100 ± 0.004 | 2.98 ± 0.01 |
| GO 2a | 21.2 ± 2.3 | 0.345 ± 0.002 | 7.7 ± 2.8 | 0.490 ± 0.090 | 10.3 ± 0.6 | 0.038 ± 0.006 | 3.5 ± 0.5 |
| GO 3b | | | | | | | 2.6 ± 0.01 |

7. Comparison of XR fit Models

Since XR data fitting is an inverse problem, it does not have a unique solution, i.e. more than one electron density profiles can satisfy the observed XR data.¹¹ Therefore it is important to use external information to limit the possibilities and obtain physically meaningful results. For the thin films at the air/water interface, it is typical to start the fit with a 1-box model representing the thin film. The subphase electron density ($0.33 e/\text{Å}^3$ for water) and electron density of air (0) are fixed parameters. The box length, electron density, and interfacial roughness parameters are allowed to vary to fit the data by minimizing a merit function. In the case of a complex film that cannot be represented by a single box, more boxes can be introduced. However, typically it is not reasonable to have a box size smaller than the resolution of the experiment, which is limited by the measured Q_{\max} .

Figure S10 and S11 show the best fits obtained by 1-Box, 2-Box, and 3-Box models for the GO-3a and GO-2a respectively. It is clear that both films require 3-boxes to represent low-electron density regions below and above the film as described in the main text. However, GO-2a can be reasonably described by 2 boxes as it is evident from the very low electron density obtained for the 3rd box towards air, in the 3-box model.

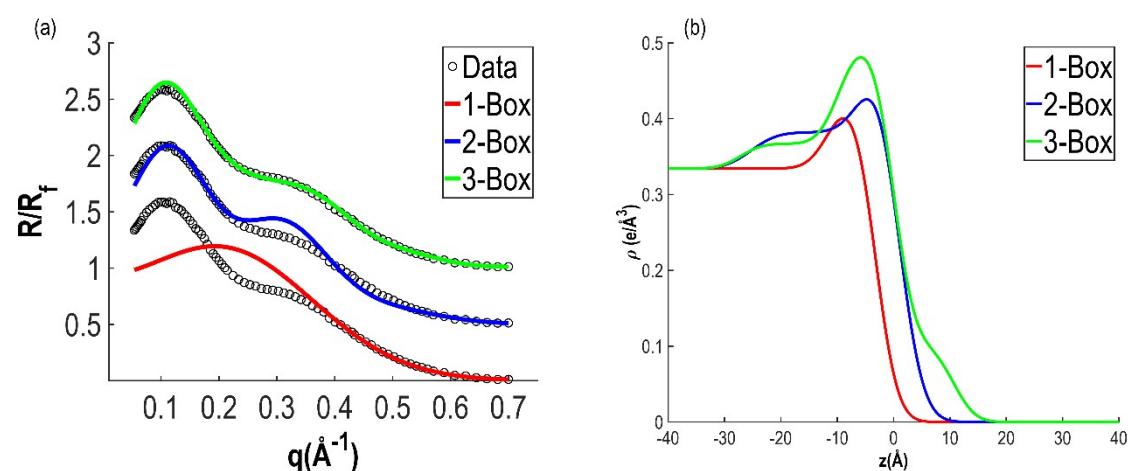


Figure S10. A comparison of XR fits (a) and corresponding electron density profiles (b) for GO-3a in Figure 3c.

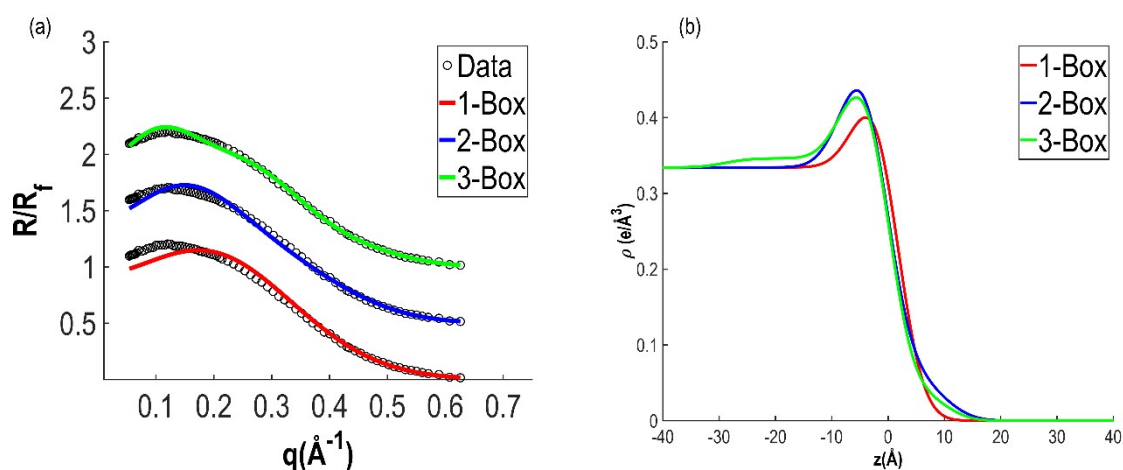


Figure S11. A comparison of XR fits (a) and corresponding electron density profiles (b) for GO-2a in Figure 3c.

References

1. Amadei, C. A.; Stein, I. Y.; Silverberg, G. J.; Wardle, B. L.; Vecitis, C. D., Fabrication and morphology tuning of graphene oxide nanoscrolls. *Nanoscale* **2016**, *8* (12), 6783-91.
2. Aldrich, S. Graphene oxide. <https://www.sigmaaldrich.com/US/en/product/aldrich/794341>.
3. Aldrich, S. Graphene oxide carboxylic acid enriched. <https://www.sigmaaldrich.com/US/en/product/aldrich/795542>.
4. Graphene, S. GO-V50. <https://standardgraphene.com/product/go-v50/>.
5. Fairley, N.; Fernandez, V.; Richard-Plouet, M.; Guillot-Deudon, C.; Walton, J.; Smith, E.; Flahaut, D.; Greiner, M.; Biesinger, M.; Tougaard, S.; Morgan, D.; Baltrusaitis, J., Systematic and collaborative approach to problem solving using X-ray photoelectron spectroscopy. *Applied Surface Science Advances* **2021**, *5*.
6. Haubner, K.; Murawski, J.; Olk, P.; Eng, L. M.; Ziegler, C.; Adolphi, B.; Jaehne, E., The route to functional graphene oxide. *Chemphyschem* **2010**, *11* (10), 2131-9.
7. Moulder, J. F.; Stickle, W. F.; Sobol, P. E.; Bomben, K. D., *Handbook of x-ray photoelectron spectroscopy*. Perkin-Elmer Corporation: Minnesota, 1992.
8. Eigler, S.; Dotzer, C.; Hof, F.; Bauer, W.; Hirsch, A., Sulfur species in graphene oxide. *Chemistry—A European Journal* **2013**, *19* (29), 9490-9496.
9. Vasile, C.; Baican, M. C.; Tibirna, C. M.; Tuchilus, C.; Debarnot, D.; Pâslaru, E.; Poncin-Epaillard, F., Microwave plasma activation of a polyvinylidene fluoride surface for protein immobilization. *J. Phys. D: Appl. Phys.* **2011**, *44* (47).
10. Amadei, C. A.; Arribas, P.; Vecitis, C. D., Graphene oxide standardization and classification: Methods to support the leap from lab to industry. *Carbon* **2018**, *133*, 398-409.
11. Pershan, P. S.; Schlossman, M., *Liquid surfaces and interfaces: synchrotron x-ray methods*. Cambridge University Press: 2012.